

Spindle error motion measurement of a large precision roll lathe

JungChul Lee[#], Wei Gao¹, Yuki Shimizu¹, Jooho Hwang², Jeong Seok Oh² and Chun Hong Park²

¹ Department of Nanomechanics, Tohoku University, Sendai, 980-8579, Japan

² Korea Institute of Machinery & Materials, Deajeon, South Korea

[#] Corresponding Author / E-mail: leejc@nano.mech.tohoku.ac.jp, TEL: +81-22-795-6953, FAX: +81-22-795-6953

KEYWORDS : Measurement, Spindle error motion; Precision lathe; Error Separation, Roll

This paper describes a spindle error motion measurement system to evaluate the performance of a spindle of a large precision roll lathe, which is under development for fabrication of large-scale roll dies of micro-structured surfaces. The measurement system employed a large-scale roll (workpiece) with a diameter of 320 mm and a length of 1800 mm as a measurement artifact instead of a master object to figure out a spindle error motion over the entire fabrication length. To separate the spindle error motion and out-of-roundness of the roll, the reversal method was employed. Two capacitive type displacement probes were mounted on the designed probe holders which were arranged to be faced to each other with the roll between them. Spindle error motion measurement was conducted at several sections of the roll along the roll axis to verify the tilt error motion of the spindle as well as the radial error motion. As the rotating speed was different for the mirror finishing fabrication of the roll and fabrication of the micro-structure on the roll, the spindle error motion was measured at different rotating speeds of 5 to 300 rpm. Experimental results of the out-of-roundness of the roll are presented as well as the spindle error motion measurement in this study.

Manuscript received: January XX, 2011 / Accepted: January XX, 2011

1. Introduction

Demands for large-scale precision roll lathes are increasing to fabricate large-scale roll dies of micro-structured surfaces in the flat panel display industry and these roll dies have been used for a roll-to-roll forming process. Micro-structures such as prism patterns are fabricated by using single point diamond cutting tools on a mirror finished surface of rolls and its machining accuracy depends on the error motions of a precision roll lathes. Because the rotating speed was different for the fabrication of the mirror finishing and micro-structure on the roll, the spindle error motion would be changed according to the rotating speed as compared with the slide error motions of the lathe.

Error separation techniques have been developed for precision measurements of the error motions without the influence of the surface form error of a measurement artifact.¹⁻⁴ In this study, for the measurement of the spindle error motions, the reversal method was employed, which gives theoretically perfect separation of the out-of-roundness to evaluate the spindle error motion if the machine has a good repeatability.²⁻⁴

This paper presents the spindle error motion measurement for next generation large precision roll lathe which is under development stage.⁵ The radial error motion and the tilt error motion are evaluated by removing of the influence of the surface form error of the artifact. The axial error motion is not concerned because this error component

is typically on the order of approximately 100 nm, thereby can be omitted in the lathe. The experiments were conducted under different rotating speeds from 5 (fabricating speed of the micro-structure on the roll) to 300 rpm (fabricating speed of the mirror finishing of the roll) to figure out the changes of the spindle error motion according to the rotating speed.

2. Measurement principle

Fig. 1 shows the schematic of the spindle error motion. The radial error motion is denoted by $e_{radial}(\theta)$ and the tilt error motion is defined as $e_{tilt}(\theta)$. The spindle error motion $e_{spindle}(z_i, \theta)$ is composed of the radial error motion $e_{radial}(\theta)$ and the tilt error motion $e_{tilt}(\theta)$. i is the

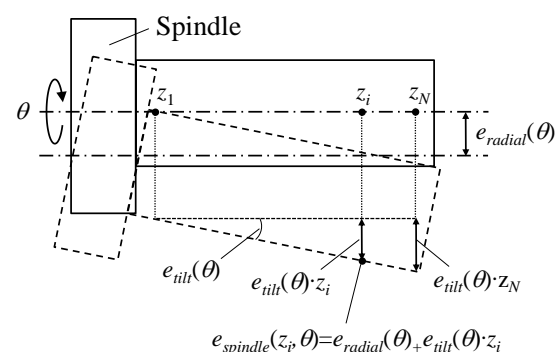


Fig. 1 Schematic of the spindle error motion

sampling number along the Z-direction. Assuming that z_1 is zero and z_N is the end Z-position of measurement, the spindle error motion can be expressed by following at a position of (z_i, θ) :

$$e_{spindle}(z_i, \theta) = e_{radial}(\theta) + e_{tilt}(\theta) \cdot z_i, \quad (i=1, \dots, N) \quad (1)$$

To figure out the spindle error motion over the entire fabrication length, both the radial error motion $e_{radial}(\theta)$ and the tilt error motion $e_{tilt}(\theta)$ should be measured.

Fig. 2 shows the measurement principle of the spindle error motion. The reversal method requires to be measured twice before and after reversal of the artifact. In the first measurement, the artifact is rotated by the spindle at the Z-position of z_i . After rotating, the Z-position is changed along the Z-direction up to the z_N . The probe outputs of the m_{A_before} and m_{B_before} at the position (z_i, θ) are denoted as follows:

$$m_{A_before}(z_i, \theta) = e_{spindle}(z_i, \theta) + R(z_i, \theta) \quad (2)$$

$$m_{B_before}(z_i, \theta) = -e_{spindle}(z_i, \theta) + R(z_i, \theta + \pi) \quad (3)$$

where $R(z_i, \theta)$ and $R(z_i, \theta + \pi)$ are the out-of-roundness at the position of (z_i, θ) and $(\theta + \pi)$, respectively.

For the second measurement, the artifact is reversed with spindle position fixed and scanned again. Assuming that the outputs of the probes after reversal are referred to as m_{A_after} and m_{B_after} , the probe outputs can be written as:

$$m_{A_after}(z_i, \theta) = e_{spindle}(z_i, \theta) + R(z_i, \theta + \pi) \quad (4)$$

$$m_{B_after}(z_i, \theta) = -e_{spindle}(z_i, \theta) + R(z_i, \theta) \quad (5)$$

The following operation can evaluate the spindle error motion without the influence of the out-of-roundness:

$$e_{spindle}(z_i, \theta) = \frac{m_{A_before}(z_i, \theta) - m_{B_after}(z_i, \theta)}{4} + \frac{m_{A_after}(z_i, \theta) - m_{B_before}(z_i, \theta)}{4} \quad (6)$$

The spindle error motion at the position of $z_i = z_1$ is the radial error motion $e_{radial}(\theta)$.

Consequently, the tilt error motion $e_{tilt}(\theta)$ can be calculated by using the obtained spindle error motions from Eq. (6) at the position of z_1 and z_N :

$$e_{tilt}(\theta) = \frac{e_{spindle}(z_N, \theta) - e_{spindle}(z_1, \theta)}{z_N - z_1} \quad (7)$$

In a way similar with Eq. (6), out-of-roundness can be obtained by following:

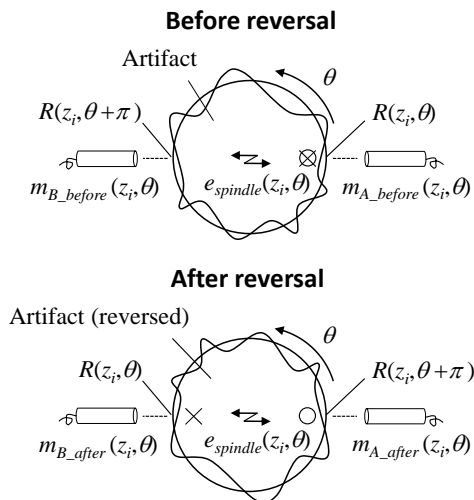


Fig. 2 Measurement principle of the spindle error motion by the reversal method

$$R(z_i, \theta) = \frac{m_{A_before}(z_i, \theta) + m_{B_after}(z_i, \theta)}{4} + \frac{m_{A_after}(z_i, \theta) + m_{B_before}(z_i, \theta)}{4} \quad (8)$$

3. Experiments

Fig. 3 shows the schematic of the measurement system. The large precision roll lathe is employed for the measurement. The spindle is driven by a frameless direct drive motor and hydrostatic bearings are employed on the headstock and the tailstock. Two capacitive type displacement probes were mounted on the designed probe holders. Probes were carefully arranged to be faced to each other (XY-plane). Two probes have a resolution of 0.5 nm and measurement range of $\pm 50 \mu\text{m} / \pm 10 \text{V}$. A copper plated hollow type roll was employed as the measurement artifact which has a diameter of 320 mm and length of 1800 mm, instead of the reference measurement artifact. Before the measurement, the roll was mirror finished (self-cut) by the diamond cutting tool with a rotating speed of 300 rpm. The weight of the roll is approximately 350 kg and deflection which was caused by own weight was approximately 20 μm . Position change due to the own weight is calculated about 1 nm. The rotary encoder gave accurate spindle position information and it can provide the trigger signal to the 16-bit DAQ module, thereby PC can sample the synchronized probe outputs.

Fig. 4 shows the measured synchronous spindle error motion at the position of $z_i = 0$ mm (i.e. the radial error motion). To identify the behavior of the spindle error motion when the roll was fabricated by the lathe, measurement speed was set to be 300 rpm which is same rotating speed of the mirror finishing fabrication. 16 revolutions were made by the spindle with a sampling interval of 2° along the circumference direction. The data are digitally filtered to 50 undulations per revolution (upr). The asynchronous error motion was 17.5 nm. The spindle error motion was evaluated approximately 200 nm under the condition of Z-position of $z_i = 0$ and rotating speed of 300 rpm, respectively. FFT analysis was also plotted and 2 upr component is dominant. Fig. 5 shows the evaluated out-of-roundness of the roll at the position of $z_i = 0$ mm and rotating speed of 300 rpm. Out-of-roundness is about 130 nm and also 2 upr component is dominant. As the roll was fabricated by the lathe, the result shows about 180° phase difference compared with the spindle error motion. As can be seen in the result of FFT, the spindle error motion was not transferred perfectly because of the wear of the diamond cutting tool and the thermal deformation between the fabrication condition and the measurement environment, etc. Fig. 6 shows the spindle error motion $e_{spindle}(z_i, \theta)$, which is composed of the radial error motion and

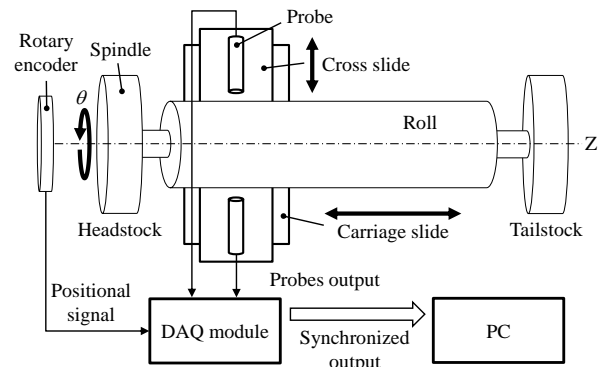


Fig. 3 Schematic of the measurement system

the tilt error motion, along the Z-axis from $z_i=0$ mm to 1700 mm. Z-directional sampling interval was set to be 100 mm. The spindle error motion is changed according to the different Z-position because of the tilt error motion. The minimum and maximum synchronous error motions are measured about 143 nm and 386 nm, respectively. Fig. 7 shows the out-of-roundness along the Z-axis at the rotating speed of 300 rpm. Minimum and maximum values are evaluated about 111 nm and 268 nm, respectively.

Measurements were also conducted at the rotating speed of 5 rpm because the fabrication rotating speed of the micro-structure on the roll surface is about 5 rpm. Fig. 8 shows the measured spindle error motion at the position of $z_i=0$ mm. The spindle error motion is totally different compared with the measurement result of 300 rpm. This result indicates that to fabricate the micro-structure precisely, spindle error motion is needed to be compensated. Fig. 9 shows the measured out-of-roundness at the position of $z_i=0$ mm and rotating speed of 5 rpm. This result is quite similar with the measurement result of 300 rpm. FFT analysis results of Fig. 5 and Fig. 9 also almost coincide contrastively to the spindle error motion. Fig. 10 shows the spindle error motion along the Z-position from $z_i=0$ mm to 1700 mm. In this case, the tilt error motion is smaller than the case of 300 rpm and it is also changed according to the rotating speed as well as the radial error motion. Fig. 11 shows the out-of-roundness along the Z-axis at the rotating speed of 5 rpm. The measurement results of at the position of $z_i=0$ mm and 1700 mm are very similar with the measurement results of 300 rpm. However, out-of-roundness values are different with measurement results of 300 rpm in the vicinity of center of roll. This phenomenon would be occurred by the deformation of the roll due to

the unbalanced mass. The roll balancing was conducted at the position of $z_i=0$ and 1700 mm. Because of this reason, measurement results at the position of $z_i=0$ mm and 1700 mm would be very similar

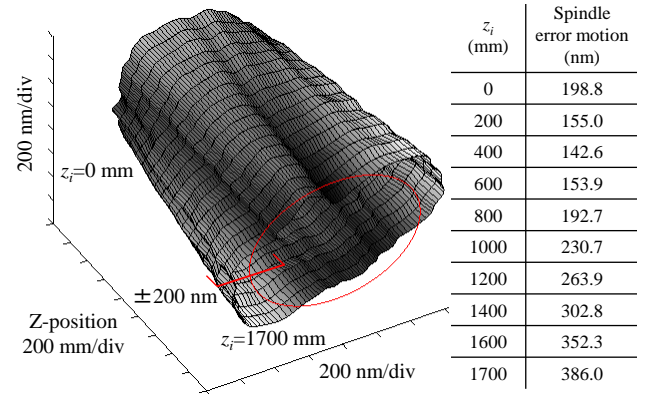


Fig. 6 Spindle error motion along the Z-axis (300 rpm)

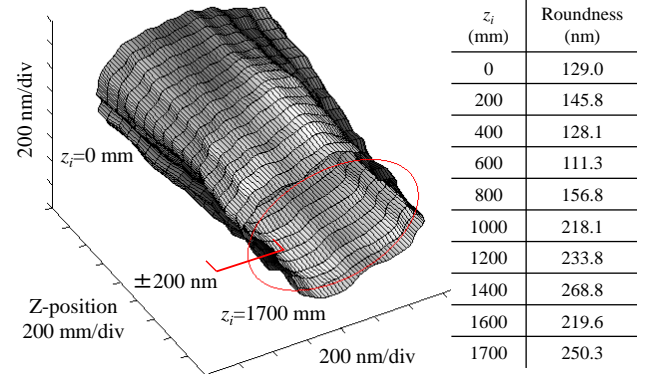


Fig. 7 Out-of-roundness of the roll along the Z-axis (300 rpm)

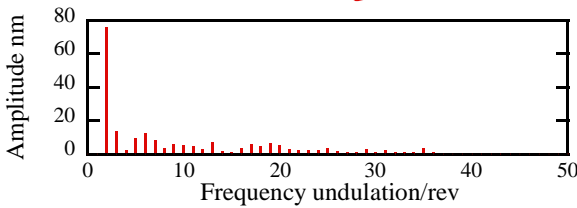
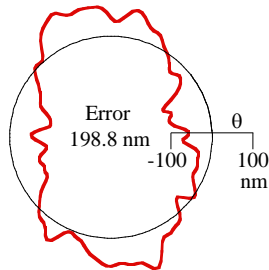


Fig. 4 Synchronous spindle error motion ($z_i=0$ mm, 300 rpm)

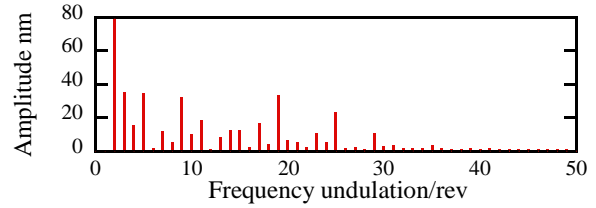
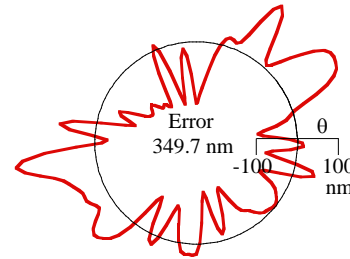


Fig. 8 Synchronous spindle error motion ($z_i=0$ mm, 5 rpm)

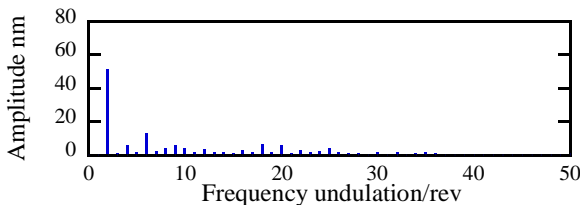
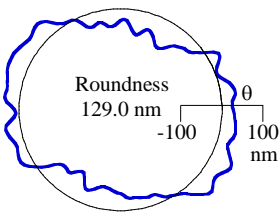


Fig. 5 Out-of-roundness of the roll ($z_i=0$ mm, 300 rpm)

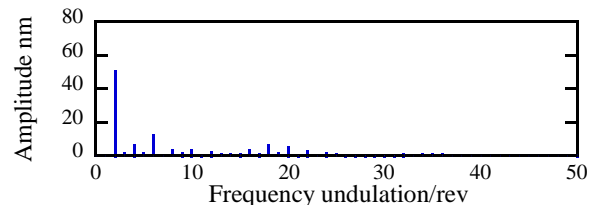
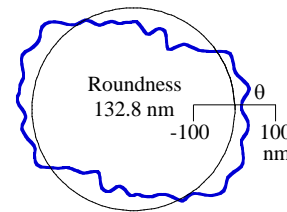


Fig. 9 Out-of-roundness of the roll ($z_i=0$ mm, 5 rpm)

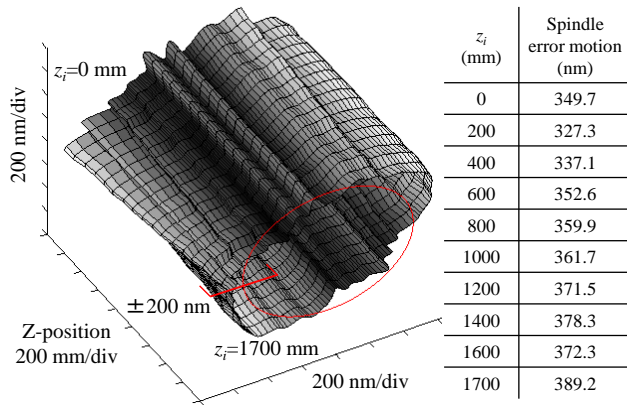


Fig. 10 Spindle error motion along the Z-axis (5 rpm)

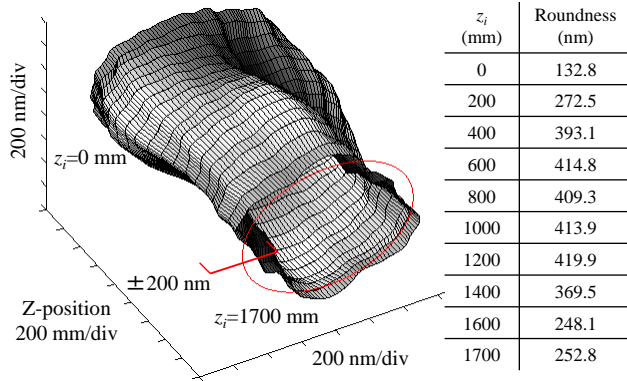


Fig. 11 Out-of-roundness of the roll along the Z-axis (5 rpm)

with the measurement results of 300 rpm.

In order to investigate changes of the spindle error motion and out-of-roundness, additional experiments were conducted under the rotating speed condition of 50, 100, 150, 200 and 250 rpm. Fig 12 shows the differences according to the rotating speed. Fig.12 (a) and (b) show the spindle error motions at the position of $z_i=0$ mm and 800 mm, respectively. The both spindle error motions at the position of $z_i=0$ and 800 mm become small according to the increasing of the rotational speed. Fig. 12 (c) and (d) show the out-of-roundness according to the rotating speed at the position of $z_i=0$ mm and 800 mm. The out-of-roundness, which were measured at the position of $z_i=0$ mm, is almost changeless. However, the out-of-roundness is changed at the position of $z_i=800$ mm according to the rotating speed, gradually.

Fig. 13 shows the evaluated tilt error motion $e_{til}(\theta)$ from Eq.(7). As can be seen in Fig. 13, the tilt error motions are different at rotating speed of 5 rpm and 300 rpm. PV values of the tilt error motion at rotating speed of 5 rpm and 300 rpm are approximately 0.04 arcsec and 0.06 arcsec. The tilt error component is important in case of the large precision lathe because it is proportional to the length.

4. Conclusions

The spindle error motion which is composed of the radial error motion and the tilt error motion is measured according to the different rotating speed on the large precision roll lathe. Two capacitive type displacement probes and roll (workpiece) are employed for the reversal method. It is figured out that the spindle error motion changes according to the rotating spindle. The out-of-roundness is also evaluated as well as the spindle error motion. The out-of-roundness is also changed except the both side section of the roll. An

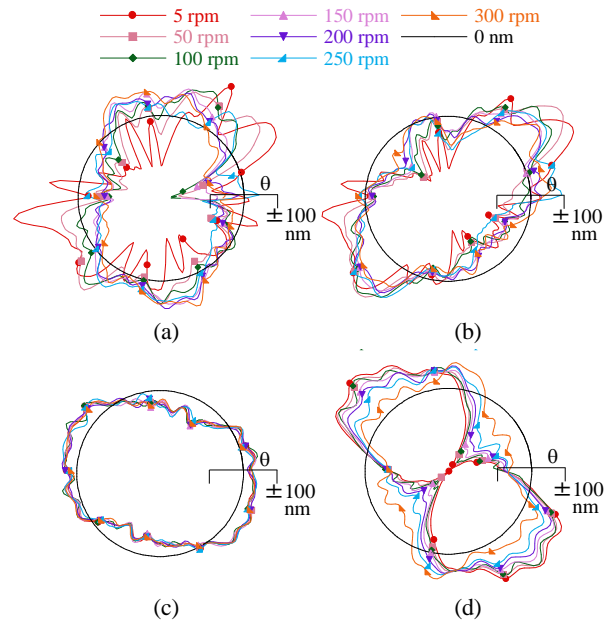


Fig. 12 (a) Differences of the spindle error motion according to the rotating speed at Z-position of $z_i=0$ mm (b) differences of the spindle error motion according to the rotating speed at Z-position of $z_i=800$ mm (c) differences of the out-of-roundness according to the rotating speed at Z-position of $z_i=0$ mm (d) differences of the out-of-roundness according to the rotating speed at Z-position of $z_i=800$ mm

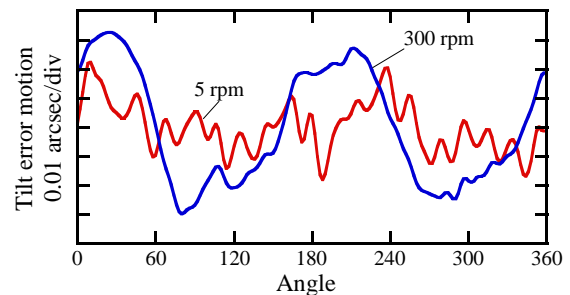


Fig. 13 Tilt error motion at rotating speed of 5 rpm and 300 rpm

analysis of the hollow type roll deformation according to the rotating speed will be carried out as a future work.

REFERENCES

- Gao, W., Kiyono, S. and Sugawara, T., "High-accuracy roundness measurement by a new error separation method," Precision Engineering, Vol. 21, pp. 123-133, 1997.
- Whitehouse, D. J., "Some theoretical aspects of error separation techniques in surface metrology," J. of Phys. E: Sci. Instrum. Vol. 9, pp. 531-536, 1976.
- Evans, C. J., Hocken, R. J. and Estler, W. T., "Self-calibration: reversal, redundancy, error separation and 'absolute testing'," Annals of CIRP, Vol. 45, No. 2, pp. 617-634, 1996.
- Gao, W., Tano, M., Araki, T., Kiyono, S. and Park, C. H., "Measurement and compensation of error motions of a diamond turning machine," Precision Engineering, Vol. 31, pp. 310-316, 2007.
- Oh, J. S., Shim, J. Y., Song, C. K. and Park, C. H., "Design and evaluation of ultra precision roll lathe for large-scale micro-structured optical films," Proceedings of the euspen International Conference, pp. 287-291, 2010.